

1-1-2011

Effect of Substrate Composition and Alignment on Corneal Cell Phenotype

Donna Phu '09
Harvey Mudd College

Lindsay S. Wray '08
Harvey Mudd College

Robert V. Warren '10
Harvey Mudd College

Richard C. Haskell
Harvey Mudd College

Elizabeth J. Orwin
Harvey Mudd College

Recommended Citation

"Effect of Substrate Composition and Alignment on Corneal Cell Phenotype", Donna Phu, Lindsay S. Wray, Robert V. Warren, Richard C. Haskell, and Elizabeth J. Orwin, *Tissue Engineering A* 17 (5-6): 799-807 (2011). DOI: 10.1089/ten.tea.2009.0724

This Article is brought to you for free and open access by the HMC Faculty Scholarship at Scholarship @ Claremont. It has been accepted for inclusion in All HMC Faculty Publications and Research by an authorized administrator of Scholarship @ Claremont. For more information, please contact scholarship@cuc.claremont.edu.

Effect of Substrate Composition and Alignment on Corneal Cell Phenotype

Donna Phu, B.S.,¹ Lindsay S. Wray, B.S.,¹ Robert V. Warren, B.S.,²
Richard C. Haskell, Ph.D.,² and Elizabeth J. Orwin, Ph.D.³

Corneal blindness is a significant problem treated primarily by corneal transplants. Donor tissue supply is low, creating a growing need for an alternative. A tissue-engineered cornea made from patient-derived cells and biopolymer scaffold materials would be widely accessible to all patients and would alleviate the need for donor sources. Previous work in this lab led to a method for electrospinning type I collagen scaffolds for culturing corneal fibroblasts *ex vivo* that mimics the microenvironment in the native cornea. This electrospun scaffold is composed of small-diameter, aligned collagen fibers. In this study, we investigate the effect of scaffold nanostructure and composition on the phenotype of corneal stromal cells. Rabbit-derived corneal fibroblasts were cultured on aligned and unaligned collagen type I fibers ranging from 50 to 300 nm in diameter and assessed for expression of α -smooth muscle actin, a protein marker upregulated in hazy corneas. In addition, the optical properties of the cell-matrix constructs were assessed using optical coherence microscopy. Cells grown on collagen scaffolds had reduced myofibroblast phenotype expression compared to cells grown on tissue culture plates. Cells grown on aligned collagen type I fibers downregulated α -smooth muscle actin protein expression significantly more than unaligned collagen scaffolds, and also exhibited reduced overall light scattering by the tissue construct. These results suggest that aligned collagen type I fibrous scaffolds are viable platforms for engineering corneal replacement tissue.

Introduction

DEVELOPMENT OF A TISSUE-ENGINEERED (TE) cornea composed of native biopolymer materials and patient-derived cells will alleviate dependency on the short supply of donor corneal tissue. Currently, the supply of viable donor tissue allows for 40,000 corneal transplants to be performed each year.¹ This donor supply is greatly outweighed by the demand for donor corneal tissue, as there are more than 10 million people throughout the world suffering from irreversible corneal blindness.² A TE cornea that incorporates patient-derived cells with a biopolymer scaffold that replicates the extracellular microenvironment of the natural cornea will be an optimal alternative to synthetic replacements and donor tissue. Successful construction of a TE cornea would also serve as an *ex vivo* platform for investigating the mechanisms of corneal blindness and human cellular responses to new ophthalmic drugs.

Corneal tissue is composed of three stratified layers: the epithelial, stromal, and endothelial layers. While each layer contributes to the overall mechanical and optical properties of the cornea, the most prominent layer is the stroma. In a healthy, transparent cornea the stromal layer is composed

of corneal keratocytes and a highly ordered configuration of extracellular matrix (ECM). Recent research has identified the importance of the intracellular protein expression of these keratocytes in maintaining corneal transparency.³⁻⁵ The keratocytes in the quiescent phenotype express two characteristic proteins: transketolase (TKT) and aldehyde dehydrogenase class 1A1 (ALDH1A1).³ A decrease in expression of TKT and ALDH1A1 expression in keratocytes leads to a marked decrease in corneal transparency and increased light scattering from keratocytes.³⁻⁵ In response to corneal wounding, the keratocytes differentiate into repair fibroblasts and eventually myofibroblasts. The myofibroblast phenotype is characterized by intracellular expression of the contractile protein α -smooth muscle actin (α -SMA).^{6,7} Induction of the myofibroblast phenotype *in vitro* and *in vivo* has been correlated to increased light scattering, which is likely due to the presence of α -SMA stress fibers.³⁻⁵ Myofibroblasts can dedifferentiate back to the quiescent phenotype upon completion of the wound-healing process *in vivo*.⁶

The other stromal component that contributes to transparency is the ECM. The stromal ECM is composed primarily of type I collagen fibers and proteoglycans.⁸ The

Departments of ¹Biology, ²Physics, and ³Engineering, Harvey Mudd College, Claremont, California.

type I collagen fibers are regularly spaced, uniformly aligned, and 25–35 nm in diameter.^{8–13} The collagen fibers are arranged parallel to each other in a 200–2,500-nm-thick lamella.^{14,15} The stromal layer contains over 300 interlaced lamellae, stacked on each other at varying angles ranging from 0° to 90°. The spatial arrangement of the small-diameter fibers in each lamella of the ECM is thought to contribute to corneal transparency.¹⁰ Thus, the disruption of the orderly arrangement of these fibers would lead to an increase in overall light-scattering of the tissue.¹⁰ A fully functional TE cornea must be able to re-create the complex and unique arrangement of the ECM because the architecture of the corneal stroma affects the optical properties of the cornea.¹⁷ Further, studies have found that the orientation of collagen fibers can affect cell behavior, such as adhesion and direction of proliferation.^{18,19} Many tissue engineers use electrospinning to replicate the fibrous nanostructure of various ECMs.²⁰ Electrospinning offers a technique for controlled fiber deposition, including fiber spacing, diameter, and orientation,²⁰ making it a promising method for engineering corneal tissue. Previous work in our lab led to the successful mimicking of the arrangement of aligned, type I collagen nanofibers in the corneal ECM using the electrospinning technique.¹⁹ Rabbit corneal fibroblasts (RCFs) were cultured on aligned and unaligned electrospun fibers, and qualitative immunofluorescence image analysis revealed not only that proliferation of RCFs was along the direction of the aligned fibers, but also that intracellular expression of α -SMA was downregulated on these aligned fibers.¹⁹ These results suggested that the corneal fibroblast phenotype is influenced by the topography and spatial arrangement of the scaffold components, which could provide a method for downregulating α -SMA expression by corneal fibroblasts cultured *in vitro*.

In this study, we assessed the effect of electrospun scaffolds on the fibroblast wound-healing phenotype and evaluated the aligned fibers as a viable scaffolding material for growing a TE cornea construct. The *in vitro* corneal stromal cell phenotype was investigated as a function of fiber density and fiber alignment. RCF intracellular expression of α -SMA was quantified by Western blot analysis. The overall light scattering of the tissue constructs was quantified with optical coherence microscopy (OCM) by measuring backscattered light. Since small-diameter, aligned fibers mimic the native corneal microstructure, we hypothesized that these scaffolds would downregulate α -SMA expression and improve optical properties of the TE construct. The results provide a basis for understanding the role of matrix structure on cell behavior, and are an important first step toward engineering transparent corneal tissue.

Methods

Electrospinning collagen nanofibers

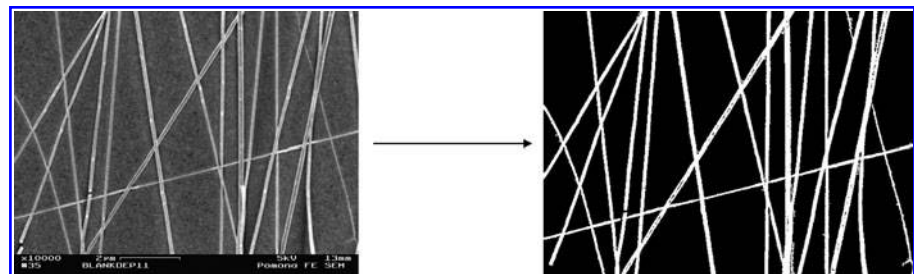
The electrospinning solution was prepared by dissolving type I collagen (acid soluble from calf skin; Elastin Products, Owensville, MO) in >99% acetic acid (EMD, San Diego, CA), as previously described.¹⁹ Initial alignment experiments used 4–7.5 wt% collagen solutions, which correspond to collagen fibers with diameters in the range of 50–451 nm. For subsequent fiber density and optical experiments, a 5 wt% collagen solution was used to obtain a measured fiber diameter of 137 ± 49 nm. All diameters were measured using scanning electron microscopy (SEM) and represent mean \pm standard deviation. Each solution was heated to 35°C for 10 to 20 min and then allowed to cool to room temperature overnight while stirring to homogenize. The solution was loaded into a 2 mL glass syringe (Air-tite Products, Germany) fitted with a blunt-ended 20 gauge needle. The syringe was then placed on a syringe pump (KD Scientific, New Hope, PA) and directed toward a grounded collection device. A high-voltage source was attached to the syringe needle. Voltages of 4.0 to 9.0 kV were applied to the needle while the flow rate on the syringe pump was set to dispense at 0.05–0.30 mL/h. The duration of electrospinning was chosen to produce a monolayer of aligned and unaligned scaffolds with consistent fiber density.

Unaligned fibers were constructed by electrospinning onto 15 mm round glass cover slips attached to a glass microscope slide backed with a grounded copper plate. Uniformly aligned fibers were constructed by electrospinning onto a dual plate device. The dual plate device consisted of two parallel 2.5 cm \times 0.5 cm copper strips attached to a quartz glass slide (McMaster-Carr, Princeton, NJ) with Gluseal, a cytocompatible glue (Glustitch, Gulf Road Point Roberts, WA). The average fiber diameter for each sample was determined by measuring 30 randomly chosen fibers with software built into the SEM (Leo 982 field emission SEM; Carl Zeiss, Peabody, MA).

Quantification of fiber density of electrospun scaffolds

Aligned and unaligned scaffolds were spun for 1, 2, or 4 min. Samples were sputter coated with gold using a Cressington 108 Auto at 40 mA for 90 s and imaged with a LEO 982 field emission SEM (Pomona College, Claremont, CA) with an acceleration voltage of 5 to 10 kV. For each sample, three SEM images were taken at 10,000 \times . The images were filtered accordingly in Adobe Photoshop 7.0 so that only white pixels represented the collagen fibers, and black pixels represented the interfiber space (Fig. 1). A histogram of the pixel contents in the filtered images provided the ratio of white pixels to total number of pixels in the image, and this

FIG. 1. SEM image of electrospun collagen scaffold (left) and the image after adjusting contrast in Adobe Photoshop 7.0 (right). In the adjusted image, the white pixels represent collagen fibers and the black pixels represent the negative space. SEM, scanning electron microscopy.



was taken as a measurement of collagen fiber density. This analysis was performed in triplicate for each condition.

Preparation of solubilized collagen gels

Collagen gel scaffolds were prepared from PureCol (Inamed, Fremont, CA) solution according to the manufacturer's protocol. In each well of a 12-well tissue culture plate, 0.3 mL of the PureCol solution was dispensed. The solution was incubated at 37°C for 45–60 min and subsequently gelled in a laminar flow hood and sterilized under ultraviolet (UV) light overnight.

Crosslinking the electrospun fibers for cell culture

All collagen scaffolds were vapor and liquid crosslinked in glutaraldehyde as described previously.¹⁹ In the case of aligned collagen fibers, the copper strips were first removed from the quartz cover slips. Scaffolds were then placed in a desiccator with 10 mL of 25% glutaraldehyde solution. After 3 days, samples were soaked in sterile 0.1% glutaraldehyde for 1 h. Scaffolds were then soaked in 0.2 M ethanolamine (Sigma Aldrich, St. Louis, MO) for 2 h to remove excess glutaraldehyde. Scaffolds were then rinsed with de-ionized water three times over 3 days and sterilized under UV light.

Culture methods for RCFs on collagen scaffolds

RCFs (P1–P6) were seeded at a density of 5,000 cells/cm² and cultured for 7 days on plastic tissue culture plates (TCP), collagen gels, and unaligned and aligned fibers. Cells were fed with normal corneal fibroblast cell growth media (NM) (Ham's nutrient mixture F-12 [DMEM-F12; Sigma, St. Louis, MO], 10% fetal bovine serum [Sigma], and 1% antibiotic/antimycotic [500 units penicillin, 0.5 µg streptomycin, 1.25 µg amphotericin B; JR Scientific, Woodland, CA]). As a positive control for α -SMA expression, RCFs were cultured on TCP and fed NM supplemented with a 2 ng/mL concentration of human transforming growth factor- β 1 (TGF- β) (NM plus 2 ng/mL of TGF- β [Sigma]) to ensure optimal upregulation of α -SMA.⁶ The medium was changed every 2–3 days.

Western blot analysis for quantifying α -SMA expression

After 7 days of culture, RCFs were prepared for Western blot analysis. Samples were trypsinized (VWR, West Chester, PA), pooled together based on media condition and scaffold type to ensure a high concentration of protein, counted in 1 mL of phosphate-buffered saline and protease inhibitor (Bio-Rad, Hercules, CA), and combined with 50 µL lysis buffer per million cells (50 mL dH₂O, 0.3 g Trizma base, 0.02 g dithiothreitol with protease inhibitor). The cells were flash-frozen in liquid nitrogen and the intracellular content was collected by centrifugation. A Bradford assay determined the protein concentration of the supernatant.

For each sample, 10 µg of protein was loaded into a 10% Bis-Tris Gel under reducing conditions (NuPAGE; Invitrogen, Carlsbad, CA). The samples were transferred to 0.2 µm nitrocellulose membranes using a dry transfer cell (Invitrogen) and nonspecific binding sites were blocked in 10% goat serum (Sigma). The membranes were sequentially incubated in primary antibody (1:200 mouse anti- α -SMA [Sigma], 1:200 mouse anti-GAPDH primary antibody [Santa Cruz Bio-

technology, Santa Cruz, CA]), and a secondary antibody [1:5000 AP-conjugated sheep anti-mouse whole molecule IgG; Sigma]). The membranes were developed with Sigmafast NBT/BCIP (Sigma) and imaged using a Bio-Rad Gel Doc XR System and Quantity One software (Bio-Rad). Relative α -SMA expression was quantified from the Western blot with a densitometric analysis tool (ImageJ; NIH, Bethesda, MD). All values for α -SMA concentration were normalized to values of glyceraldehyde 3-phosphate dehydrogenase (GAPDH) to control for protein loading. For assessment of α -SMA expression of RCFs cultured on different substrate materials, the α -SMA bands were normalized to the NM TCP sample in addition to normalization to GAPDH to control for blot intensity differences due to experimental variation during blot development. The value for the NM TCP sample was found to be significantly consistent among all Western blots analyzed.

OCM preparation and imaging

OCM produces three-dimensional (3D) images of tissue based on the amount of backscattered light at each volume element (voxel). The OCM instrument and analysis software were developed at Harvey Mudd College.²¹ After 7 days of cell culture, samples were fixed in neutral buffered formalin (VWR, West Chester, PA) and stored overnight at 4°C. Samples were rinsed and submerged in phosphate-buffered saline and mounted on a glass microscope slide tilted at 19° from normal. This setup was designed to avoid the specular reflection from the microscope slide and sample substrates. For each sample, a 500×500 µm (field of view)×300 µm (deep) image was acquired and analyzed with visualization software (AVS Visualization Express 6.0, Waltham, MA) to measure the amount of backscattered light normalized by the volume of the image (total number of voxels). OCM images were acquired at three different sample sites for each of nine samples of each culture condition.

Statistical analysis

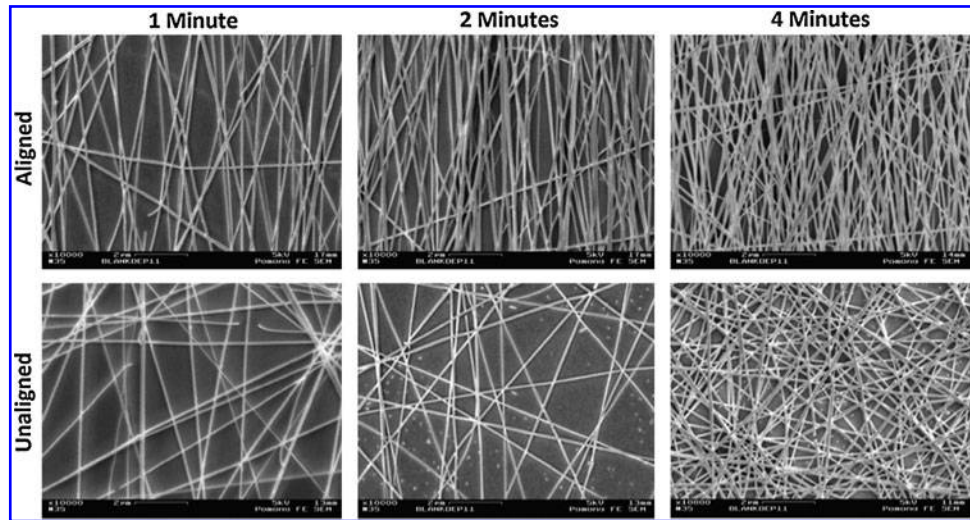
The paired Student's *t*-test assessed significant differences in all data. Data were considered significant for $p < 0.05$. Fiber diameter ranges were reported as mean \pm standard deviation. All other data were reported as the mean \pm standard error.

Results

Fiber density in aligned and unaligned electrospun scaffolds

To ensure that aligned and unaligned scaffolds had the same amount of collagen content, the fiber density of both types of electrospun scaffold was investigated as a function of electrospinning time. When the electrospinning duration was held constant, the aligned scaffolds (Fig. 2, top row) consistently contained significantly higher fiber densities than the unaligned scaffolds (Fig. 2, bottom row) ($p < 0.04$). This discrepancy is most likely due to the difference of collection plate configurations between aligned and unaligned scaffolds. However, aligned scaffolds spun for 2 min and unaligned scaffolds spun for 4 min had similar fiber densities of 0.44 ± 0.04 and 0.40 ± 0.02 , respectively ($p > 0.11$), as did aligned scaffolds spun for 1 min and unaligned scaffolds

FIG. 2. SEM images of electrospun aligned (top row) and unaligned (bottom row) fibers spun for 1 min (left column), 2 min (middle column), and 4 min (right column). All images were taken at 10,000 \times .



spun for 2 min ($p > 0.11$) (Table 1). All subsequent cell culture experiments used aligned and unaligned fibrous scaffolds that had been electrospun for 2 and 4 min, respectively. Aligned scaffolds electrospun for 2 min and unaligned scaffolds electrospun for 4 min are referred to as the high-density scaffolds. Aligned and unaligned scaffolds spun for 1 min are referred to as the low-density scaffolds.

Effect of fiber density on α -SMA expression

RCFs were cultured on aligned and unaligned scaffolds with high fiber density (high-density scaffolds) and compared to RCFs cultured on aligned and unaligned scaffolds with low fiber density (low-density scaffolds) (Fig. 3). Aligned and unaligned high-density scaffolds, respectively, had collagen contents of 0.44 ± 0.04 and 0.40 ± 0.02 . Aligned and unaligned low-density scaffolds, respectively, had collagen contents of 0.36 ± 0.02 and 0.27 ± 0.02 . RCFs cultured on high-density scaffolds exhibited lower levels of α -SMA expression than on low-density scaffolds ($p < 0.0008$) in each of the two cases—aligned and unaligned scaffolds. Additionally, the aligned fibers downregulated levels of cellular α -SMA expression compared to unaligned fibers ($p < 0.03$) in each of the two cases—high- and low-density scaffolds (Fig. 3).

Effect of alignment on α -SMA expression

Aligned scaffolds reduced α -SMA expression levels by an average of $28\% \pm 5\%$ over unaligned scaffolds for all three fiber diameter ranges studied (Fig. 4). No definitive trend was determined in α -SMA expression with fiber diameter,

but this will be the topic of future investigations. To determine the effect of alignment alone on α -SMA expression, aligned and unaligned scaffolds of intermediate diameter (137 ± 49 nm) were controlled for fiber density and re-assessed for the effects of scaffold orientation on α -SMA expression. (Fig. 3). The results showed that aligned fibers significantly decrease cellular α -SMA expression compared to unaligned scaffolds, collagen gels, and TCP ($p < 0.01$)

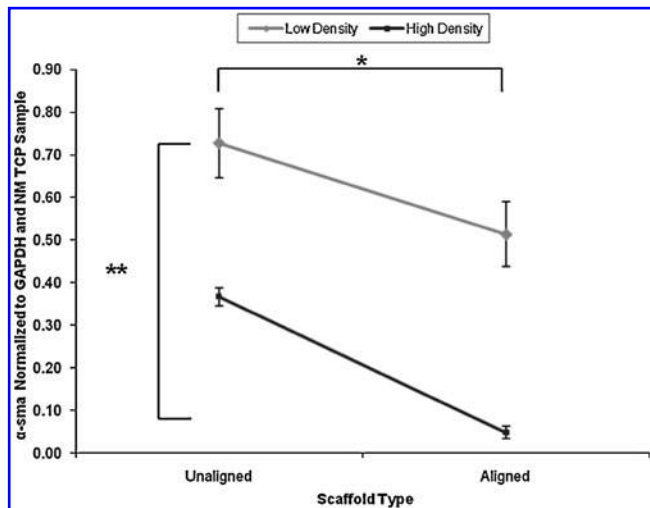


FIG. 3. Ratio of α -SMA to GAPDH for RCFs cultured on aligned and unaligned collagen scaffolds with high and low densities. Data represent mean \pm standard error with $n = 3$ for high density trials and $n = 13$ for low density trials. A paired comparison between aligned and unaligned scaffolds in each of the two cases—high and low density—showed that alignment of collagen fibers significantly downregulated α -SMA ($*p < 0.03$). Another paired comparison between high- and low-density scaffolds in each of the two cases—aligned and unaligned fibers—showed that high density of fibers is also an important factor in downregulating α -SMA ($**p < 0.0008$). α -SMA, α -smooth muscle actin; GAPDH, glyceraldehyde 3-phosphate dehydrogenase; RCF, rabbit corneal fibroblasts; NM, normal corneal fibroblast cell growth media; TCP, tissue culture plates.

TABLE 1. COLLAGEN DENSITY OF ELECTROSPUN SCAFFOLDS (MEAN \pm STANDARD ERROR)

	Aligned	Unaligned
1 min	0.36 ± 0.02^a	0.27 ± 0.02
2 min	0.40 ± 0.03^b	0.33 ± 0.01^a
4 min	0.56 ± 0.02	0.40 ± 0.02^b

^{a,b} $p > 0.11$; all other paired comparisons yielded p -values < 0.04 .

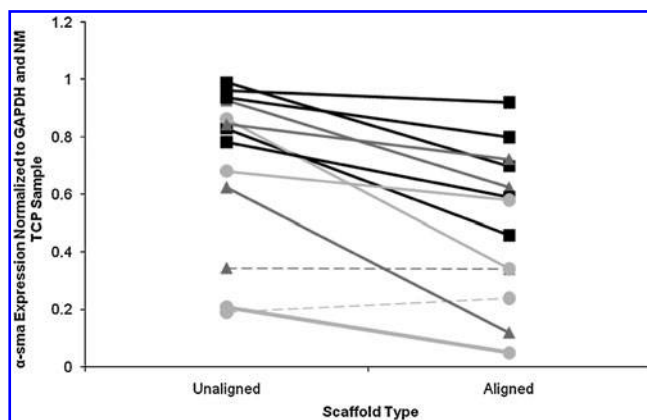


FIG. 4. Paired analysis of α -SMA expression for each unaligned versus aligned trial across different fiber diameter ranges. A total of 13 independent trials were analyzed. The gray triangles represent trials on fiber diameters of 89 ± 39 nm ($n=4$), black squares on fiber diameters of 140 ± 58 nm ($n=5$), and gray circles on fiber diameters of 358 ± 93 nm ($n=4$). The solid lines represent trials in which the RCFs cultured on aligned fibers exhibited a downregulation in α -SMA expression compared to the unaligned samples. The dashed lines represent the two trials in which the RCFs cultured on aligned fibers exhibited an up-regulation or no change in α -SMA expression compared to the unaligned samples. The expression levels of α -SMA normalized to GAPDH varied between each trial, but in 11 of the 13 trials a decrease was observed between the unaligned and aligned samples (11 paired comparisons yielded $*p < 0.01$).

(Figs. 5 and 6). RCFs cultured on TCP expressed the highest levels of α -SMA expression, with the TGF- β sample expressing more than the NM sample ($p < 0.001$). Collagen gel samples expressed less α -SMA than the TCP samples ($p < 0.05$) but expressed more α -SMA than both unaligned and aligned collagen fiber samples ($p < 0.009$) (Fig. 6).

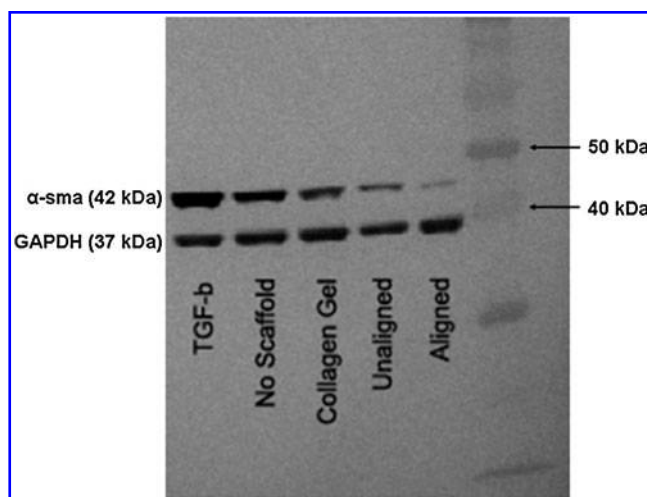


FIG. 5. Representative Western blot of RCFs cultured on aligned scaffolds, unaligned scaffolds, collagen gels, no scaffolds (TCP), and in TGF- β -supplemented media for 1 week. Blots were stained for α -SMA and GAPDH. TGF- β , transforming growth factor.

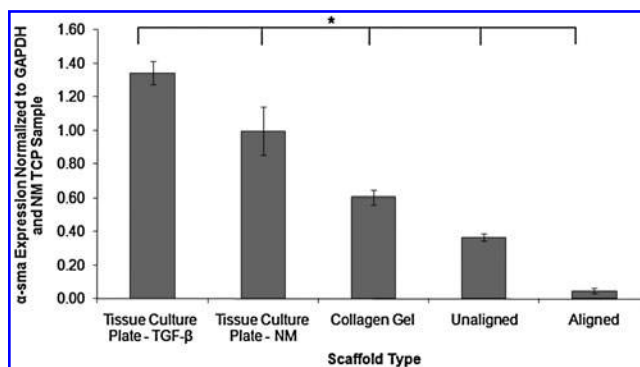


FIG. 6. Expression levels of α -SMA normalized to GAPDH and NM TCP sample for RCFs cultured for 7 days on TCP with TGF- β , TCP with NM media, collagen gels, unaligned scaffolds, and aligned scaffolds. Protein expression was quantified with Western blot analysis. Data represent mean \pm standard error with $n=3$ for each condition. Levels of α -SMA expression for each culture condition was found to be statistically different from each other ($*p < 0.05$).

Effect of alignment on optical properties of cell-seeded scaffolds

The overall light-scattering properties of cell-seeded scaffolds were quantified with backscattered light measurement using OCM. RCFs cultured on TCP scattered less light than RCFs cultured on TCP supplemented with TGF- β as a positive control (Fig. 7). For the cultures using a collagen scaffold, light scattering was greatest in collagen gel samples, then unaligned samples, and then aligned samples ($p < 0.05$).

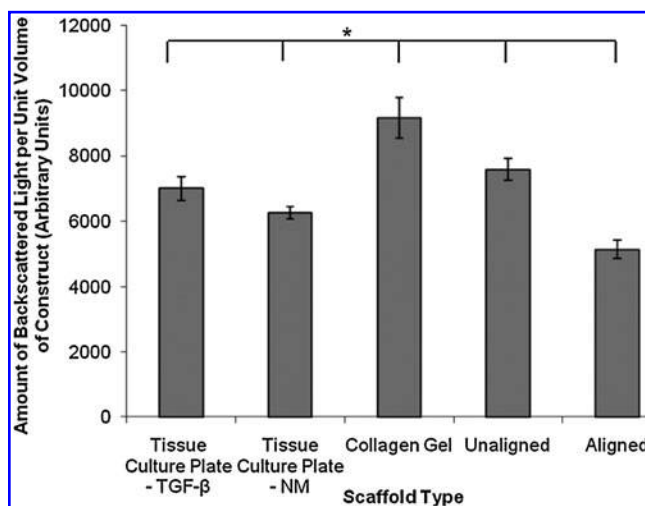


FIG. 7. Amount of backscattered light per unit volume of construct measured using the optical coherence microscopy. Culture conditions include RCFs grown on TCP with TGF- β media and NM, collagen gels, unaligned, and aligned scaffolds. For each culture condition, three images were taken of each of nine samples, and backscattered light measurements were averaged over the three images to form a data point for each of the nine samples. Data represents mean \pm standard error with $n=9$ for each condition. Amount of backscattered light was significantly different for all culture conditions ($*p < 0.05$).

(Fig. 7). Corneal cells cultured on aligned collagen scaffolds scattered less light than all other scaffolds tested ($p < 0.05$) (Fig. 7).

Matrix secretion by RCFs on different substrates

Previous studies have shown that RCFs grown on aligned substrates aligned themselves along the direction of fiber orientation.¹⁹ In this study, we used SEM to assess the morphology of the ECM deposited by the RCFs that were cultured on different substrates (Fig. 8). The micrographs confirmed that the RCFs (indicated by "C" symbol) were able to proliferate along the direction of the aligned fibers. Further, an ECM containing a high number of fibrous patches of 30–50 nm fibers (indicated by "*" symbol) was observed on cells grown on aligned and unaligned electrospun samples. In contrast, RCFs cultured on TCP secreted an ECM that contained only regions of a sponge-structured matrix, as indicated by the "ε" symbol (Fig. 8). None of the TCP samples thus far showed any evidence that a fibrous ECM was laid down by the RCFs. The substrate material appeared to have an effect only on the morphology of the ECM laid down by RCFs, and not on the amount of ECM laid down.

Discussion

Scaffold composition affects cell phenotype

This study has shown that a collagenous scaffold can affect cell behavior. Several studies have illustrated the importance of selecting an appropriate substrate material for TE applications, as many synthetic polymers have been shown to be cytotoxic and induce inflammatory responses from the cells.²⁰ One study found that human embryonic palatal mesenchymal cells exhibited greater proliferation and adhesion on electrospun fibrous scaffolds made of various natural polymers, including collagen, over standard TCP.²² These findings support the hypothesis that the che-

mical composition of substrate materials can influence cell behavior.

To investigate the differential effects of substrate composition and substrate structure, the electrospun scaffolds of different fiber densities were prepared for RCF culture and the levels of intracellular α -SMA were measured with Western blot analysis. The results showed that culturing cells on collagen scaffolds can significantly reduce α -SMA expression over culturing on standard TCP (Fig. 6). Corneal cells cultured on high-density scaffolds also expressed significantly less α -SMA than those cultured on low-density scaffolds, correlating increased collagen content with decreased α -SMA expression (Fig. 3). Our findings showed that collagen can induce cells to downregulate α -SMA, which is indicative of the reversal from the myofibroblast to the repair fibroblast phenotype. Therefore, type I collagen may be an important signal in mediating the transition between RCF phenotypes. These results support the hypothesis that substrate composition not only affects cell viability, as has been shown in other studies, but can also influence other important aspects of cell behavior such as intracellular protein expression.^{20,23} It should be reiterated that the presented investigations are of fibroblasts seeded on a monolayer of collagen fibers. Future studies will involve an expansion into a 3D study with thicker, multilayer scaffolds of collagen fibers to begin optimizing the reconstruction of a TE cornea.

Scaffold alignment is an important cell signal

In this study, we demonstrate that scaffold alignment provides an important signal to corneal cells. The ability of corneal keratocytes to alter their behavior in response to the topographic cues has been well characterized in other studies. In particular, one study reported the use of synthetic silicon wafers with micro- and nanosize grooves to align corneal keratocytes in one direction.²⁴ Keratocytes were able to respond more efficiently to substrate topography than

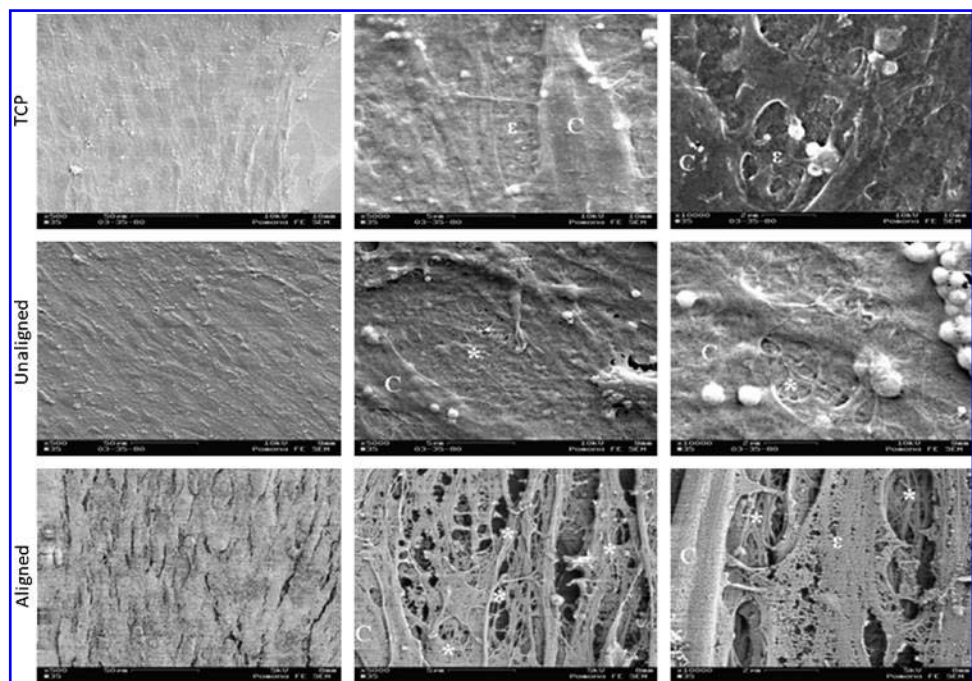


FIG. 8. SEM images of RCF constructs cultured on TCP (top), unaligned (middle), and aligned (bottom). Images are taken at increasing magnitudes from left to right. All cell bodies are labeled with "C." Sponge-like extracellular matrices are labeled with "ε," and small, 30–50 nm fibers are labeled with "*."

epithelial cells because keratocytes experience similar topographic cues *in vivo* as they are embedded in layers of aligned type I collagen fibers in the natural stroma. Another group found that the groove and ridge template structure can also control the orientation of type I collagen and keratan sulfate as they are secreted from human corneal keratocytes.²⁵ Additionally, UV-visible spectrophotometer scans of keratocyte cultures showed that keratocytes cultured on patterned substrates led to constructs that were more transparent than those cultured on unpatterned substrates of the same material.²⁵ These findings suggest that an aligned scaffolding material may influence corneal fibroblast behavior to not only express a less light-scattering cellular phenotype and but also secrete a more organized ECM, which are two ideal properties of a TE cornea construct.

In our study, we showed with Western blot analysis that aligned fibers significantly downregulate α -SMA protein expression in RCFs compared to the unaligned fibers and to collagen gels after 7 days in culture in serum-containing media ($p < 0.01$) (Figs. 4 and 6). Fiber alignment played a significant role in controlling the fibroblast phenotype and substantiates the hypothesis that myofibroblasts are not terminally differentiated, which was first questioned by Wilson *et al.*²⁶ Previous *in vitro* studies have demonstrated the reversibility of myofibroblasts back to repair fibroblasts cultured in serum using soluble factors such as fibroblast growth factor and blocking antibodies of TGF- β .^{27–29} Here, we have demonstrated the same reversible pathway using aligned type I collagen fibers as a topographical cue to effectively reduce levels of α -SMA, and consequently the myofibroblastic phenotype, nearly to zero after 7 days of culture in serum-containing media. Further, our results provide evidence that mimicking both the biochemical and physical structure of the cell substrate will be the first step in the reconstruction of a viable cornea tissue equivalent.

Optical properties and intracellular protein expression

In this study, we were also able to correlate intracellular protein expression and macroscopic optical properties of the tissue. Previous studies have focused on the cellular components that contribute to corneal haze and make a connection between the myofibroblast phenotype and increased light scattering. Through slit-lamp biomicroscopy and *in vivo* confocal microscopy, clinical studies have shown an increase in corneal opacity and reflectivity in patients with recently damaged cornea tissue.^{4,30} These studies demonstrated that the principal cause of loss of transparency in the corneas of all these patients was an increase in light scattering from the differentiation of stromal keratocytes into myofibroblasts.^{4,30} More recent studies have induced the myofibroblast phenotype using TGF- β and reported increased light scattering in myofibroblasts over corneal keratocytes cultured in serum-free media *in vitro*.⁵ In all of these studies, it is hypothesized that the elevated light-scattering property of the myofibroblastic phenotype is due to the presence of α -SMA stress fibers; however, this hypothesis has not been extensively investigated.

This study is the first to simultaneously study levels of α -SMA expression and optical properties induced by growth of RCFs on aligned scaffolds. In our study, Western blotting and OCM were used to investigate how reduced levels of

α -SMA correspond to the overall scattering properties of each construct. These studies demonstrated a distinct correlation between intracellular α -SMA expression and light scattering of the tissue constructs cultured on a scaffolding material other than TCP. The highest light scattering and α -SMA expression was found in the collagen gel samples, followed by the unaligned samples, and then the aligned samples with the lowest α -SMA and least light scattering (Figs. 6 and 7). Interestingly, RCFs cultured on TCP scattered less light than those cultured on collagen gels and unaligned samples even though these cultures expressed the highest levels of α -SMA from the Western blot analysis (Figs. 6 and 7). Light scattering can be affected by the cellular phenotype, the scaffolding templates, and any ECM that the cells deposit during the culture period. Our results suggest that the alignment of the substrate material not only reduces light-scattering proteins, but may also induce fibroblasts to secrete and remodel an ECM structure that enhances optical properties. Preliminary results in our lab have indicated that the scaffolding templates themselves contribute minimally to the overall tissue light scattering (data not shown), indicating that the scattering comes predominantly from the cells or from matrix secreted by the cells during culture. Therefore, it is likely that the scaffolding template material may be inducing RCFs to deposit ECMs of different physical and chemical structure, which will affect the optical properties of the overall tissue construct despite intracellular α -SMA expression levels. One research group demonstrated that the microstructure of a cell culture substrate can influence the morphology of the ECM deposited by human corneal keratocytes (HCKs). HCKs cultured on collagen films promoted HCKs to deposit smaller-diameter fibers than HCKs cultured on 1–2 μ m microgrooved films.³¹ In addition, they showed that the length of culture time can affect ECM morphology. HCKs were found to secrete more mesh-like structures after 2 weeks of culture time.³¹ SEM analysis of our samples has indicated different matrix structures produced by RCFs on TCP and RCFs on fibrous, collagen scaffolds (Fig. 8). RCFs cultured on TCP secreted ECM that was sponge-like in structure, where as those cultured on fibrous scaffolds secreted ECM that contained patches of small-diameter fibers of 30–50 nm. Crabb *et al.* identified similar mesh-like ECM structures in their cultures and confirmed these to be fibronectin, which is a common ECM protein found in wound-healing phenotypes.³¹ Additionally, other research groups have attributed loss of transparency to a decreased organization of the ECM of their tissue constructs.²⁵ The differences in ECM morphology may explain why RCFs cultured on TCP scatter less light than those on unaligned samples despite the fact that RCFs express more α -SMA when cultured on TCP. However, it is promising to observe that the aligned samples had the least light scattering of all culture conditions, even including the TCP samples, despite differences in secreted ECM morphology. Further work using the SEM and OCM to rigorously characterize ECM morphology and analyze its light scattering properties must be conducted to determine the differential effects between light scattering due to cellular phenotype and that due to organization of the ECM.

In general, increased expression of intracellular α -SMA in our constructs correlated with increased light-scattering properties, which supports the literature that describes

α -SMA as a contractile protein that contributes to corneal haze during the wound healing process.⁵ OCM provides information about the light-scattering properties of the overall tissue construct, and not just from individual keratocytes. Therefore, OCM allows us to assess the amount of light scattering contributed from the keratocytes, the scaffolding material, and the interactions between the keratocytes and the secreted ECM. This is useful for obtaining information about global properties of a TE construct. Overall, these studies are able to demonstrate alignment as an important cell signal for downregulating α -SMA and then directly link low α -SMA expression levels to the enhanced optical properties of the construct.

Conclusions

In summary, significant progress was made toward recreating the microenvironment of the stromal ECM in the native cornea. This study demonstrated the importance of the physical and biochemical properties of the scaffolding material in influencing fibroblast behavior. Collagen type I downregulated α -SMA, but alignment had an even more significant downregulating effect. Most importantly, we have shown that aligned collagen scaffolds not only dedifferentiated cells from the myofibroblast phenotype, but also improved the optical properties of the tissue construct. Although groups have shown separately that there are links between scaffold alignment and construct transparency and between cell phenotype and transparency, no group has cohesively incorporated the effects of cellular contribution and scaffold alignment on the light-scattering properties of a TE cornea model. The corneal biology research community has established a link between the myofibroblast phenotype and corneal haze, which is hypothesized to be due to α -SMA stress fibers,^{4,5,30} but there have not been many studies on the effect of α -SMA on the function of a TE cornea. The strong clinical evidence supporting a correlation between corneal haze and α -SMA expression indicates that α -SMA has a potentially important contribution to the light-scattering properties of a TE cornea model. However, future studies on the presence of TKT and ALDH1A1 will be important to identify the normal quiescent phenotype and conclude whether an aligned scaffold is necessary for maintaining transparency in an engineered cornea construct. This study provides important evidence for the consideration of substrate structure as well as substrate composition when designing a TE cornea. Future work will involve extensively studying the effect of substrate organization on the various properties of tissue constructs, such as cell phenotype, ECM deposition, and light scattering, as well as expansion of studies into a 3D culture environment. Nonetheless, the findings obtained from these experiments provide useful knowledge for continuing studies to engineer a viable cornea tissue equivalent.

Acknowledgments

The authors thank the Arnold and Mabel Beckman Family Foundation and the Engman Fellowship Program at Harvey Mudd College for their financial support. The authors also thank the assistance of Dr. S. Adolph, E. Guerra, I. Wulur, S. Sun, and N. Esclamado from the Harvey Mudd Biology Department and bioSTAR West in Claremont, CA.

Disclosure Statement

No competing financial interests exist.

References

1. Cornea donation & transplantation statistics. Eye Bank Association of America. www.restoreight.org/donation/statistics.htm. Accessed May 19, 2009.
2. Langer, R., and Vacanti, J.P. *Tissue Eng Sci* **260**, 920, 1993.
3. Jester, J.V., Moller-Pedersen, T., Huang, J., Sax, C.M., Kays, W.T., Cavanagh, H.D., Petroll, W.M., and Piatigorsky, J. The cellular basis of corneal transparency: evidence for 'corneal crystallins'. *J Cell Sci* **112(Pt 5)**, 613, 1999.
4. Jester, J.V. Corneal crystallins and the development of cellular transparency. *Semin Cell Dev Biol* **19**, 82, 2008.
5. Jester, J.V., Budge, A., Fisher, S., and Huang, J. Corneal keratocytes: phenotypic and species differences in abundant protein expression and *in vitro* light-scattering. *Invest Ophthalmol Vis Sci* **46**, 2369, 2005.
6. Jester, J.V., Petroll, W.M., Barry, P.A., and Cavanagh, H.D. Expression of alpha-smooth muscle (alpha-SM) actin during corneal stromal wound healing. *Invest Ophthalmol Vis Sci* **36**, 809, 1995.
7. Fini, M.E. Keratocyte and fibroblast phenotypes in the repairing cornea. *Prog Retin Eye Res* **18**, 529, 1999.
8. Ihanamaki, T., Pelliniemi, L.J., and Vuorio, E. Collagens and collagen-related matrix components in the human and mouse eye. *Prog Retin Eye Res* **23**, 403, 2004.
9. Cox, J.L., Farrell, R.A., Hart, R.W., and Langham, M.E. The transparency of the mammalian cornea. *J Physiol* **210**, 601, 1970.
10. Komai, Y., and Ushiki, T. The three-dimensional organization of collagen fibrils in the human cornea and sclera. *Invest Ophthalmol Vis Sci* **32**, 2244, 1991.
11. Benedek, G. Theory of transparency of the eye. *Appl Opt* **10**, 459, 1971.
12. Muller, L.J., Pels, E., Schurmans, L.R., and Vrensen, G.F. A new three-dimensional model of the organization of proteoglycans and collagen fibrils in the human corneal stroma. *Exp Eye Res* **78**, 493, 2004.
13. Maurice, D.M. The structure and transparency of the cornea. *J Physiol* **136**, 263, 1957.
14. Radner, W., and Mallinger, R. Interlacing of collagen lamellae in the midstroma of the human cornea. *Cornea* **21**, 598, 2002.
15. Linsenmayer, T.F., Fitch, J.M., Gordon, M.K., Cai, C.X., Igoe, F., Marchant, J.K., and Birk, D.E. Development and roles of collagenous matrices in the embryonic avian cornea. *Prog Retin Eye Res* **17**, 231, 1998.
16. Meek, K.M., and Boote, C. The organization of collagen in the corneal stroma. *Exp Eye Res* **78**, 503, 2004.
17. Shah, A., Brugano, J., Sun, S., Vase, A., and Orwin, E.J. The development of a tissue-engineered cornea: biomaterials and culture methods. *Pediatr Res* **63**, 535, 2008.
18. Pham, Q.P., Sharma, U., and Mikos, A.G. Electrospinning of polymeric nanofibers for tissue engineering applications: a review. *Tissue Eng* **12**, 1197, 2006.
19. Wray, L.S., and Orwin, E.J. Recreating the microenvironment of the native cornea for tissue engineering applications. *Tissue Eng Part A* **15**, 1463, 2009.
20. Sill, T.J., and von Recum, H.A. Electrospinning: applications in drug delivery and tissue engineering. *Biomaterials* **29**, 1989, 2008.
21. Hoeling, B.M., Fernandez, A.D., Haskell, R.C., Huang, E., Myers, W.R., Petersen, D.C., Ungersma, S.E., Wang, R., and Williams, M.E. An optical coherence microscope for

- 3-dimensional imaging in developmental biology. *Opt Express* **6**, 136, 2000.
22. Li, M., Mondrinos, M.J., Ghandi, M.R., Ko, F.K., Weiss, A.S., and Lelkes, P.I. Electrospun protein fibers as matrices for tissue engineering. *Biomaterials* **26**, 5999, 2005.
 23. Chen, F., Li, X., Mo, X., He, C., Wang, H., and Ikada, Y. Electrospun chitosan-P(LLA-CL) nanofibers for biomimetic extracellular matrix. *J Biomater Sci Polymer Edn* **19**, 677, 2008.
 24. Teixeira, A.L., Nealey, P.F., and Murphy, C.J. Responses of human keratocytes to micro- and nanostructured substrates. *J Biomed Mater Res* **71A**, 369, 2004.
 25. Vrana, E., Builles, N., Hindie, M., Damour, O., Aydinli, A., and Hasirci, V. Contact guidance enhances quality of tissue engineered corneal stroma. *J Biomed Mat Res* **84A**, 454, 2007.
 26. Wilson, S.E., Mohan, R.R., Mohan, R.R., Ambrosio, R., Jr., Hong, J., and Lee, J. The corneal wound healing response: cytokine-mediated interaction of the epithelium, stroma, and inflammatory cells. *Prog Ret Eye Res* **20**, 625, 2001.
 27. Maltseva, O., Folger, P., Zekaria, D., Petridou, S., and Masur, S.K. Fibroblast growth factor reversal of the cornea myofibroblast phenotype. *Invest Ophthalmol Vis Sci* **42**, 2490, 2001.
 28. West Mays, J.A., and Dwivedi, D.J. The keratocyte: corneal stromal cell with variable repair phenotypes. *J Biochem Cell Bio* **38**, 1625, 2006.
 29. Jester, J.V., Barry-Lane, P.A., Petroll, W.M., Olsen, D.R., and Cavanaugh, H.D. Inhibition of corneal fibrosis by topical application of blocking antibodies to TGF- β in the rabbit. *Cornea* **16**, 177, 1997.
 30. Moller-Pedersen, T. Keratocyte reflectivity and corneal haze. *Exp Eye Res* **74**, 553, 2004.
 31. Crabb, R.A.B., Chau, E.P., Decoteau, D.M., and Hubel, A. Microstructural characteristics of extracellular matrix produced by stromal fibroblasts. *Ann Biomed Eng*, **34**, 1615, 2006.

Address correspondence to:

Elizabeth J. Orwin, Ph.D.

Department of Engineering

Harvey Mudd College

301 Platt Blvd.

Claremont, CA 91711

E-mail: orwin@hmc.edu

Received: November 06, 2009

Accepted: October 21, 2010

Online Publication Date: November 30, 2010

This article has been cited by:

1. Russell E. Thompson, Liana C. Boraas, Miranda Sowder, Marta K. Bechtel, Elizabeth J. Orwin. 2013. Three-Dimensional Cell Culture Environment Promotes Partial Recovery of the Native Corneal Keratocyte Phenotype from a Subcultured Population. *Tissue Engineering Part A* **19**:13-14, 1564-1572. [[Abstract](#)] [[Full Text HTML](#)] [[Full Text PDF](#)] [[Full Text PDF with Links](#)]
2. Sahar Salehi, Mohammadhossein Fathi, Shaghayegh Haghjooy Javanmard, Thomas Bahners, Jochen S. Gutmann, Süleyman Ergün, Klaus P. Steuhl, Thomas A. Fuchsluger. 2013. Generation of PGS/PCL Blend Nanofibrous Scaffolds Mimicking Corneal Stroma Structure. *Macromolecular Materials and Engineering* n/a-n/a. [[CrossRef](#)]
3. Alexander R. Nectow, Misha E. Kilmer, David L. Kaplan. 2013. Quantifying cellular alignment on anisotropic biomaterial platforms. *Journal of Biomedical Materials Research Part A* n/a-n/a. [[CrossRef](#)]
4. Amy P. Lynch, Mark Ahearne. 2013. Strategies for developing decellularized corneal scaffolds. *Experimental Eye Research* **108**, 42-47. [[CrossRef](#)]
5. Yanming Wang, Shidong Jiang, Haigang Shi, Wei Zhang, Jing Qiao, Man Wu, Ye Tian, Zhongwei Niu, Yong Huang. 2013. Hetero-epitaxy of anisotropic polycaprolactone films for the guidance of smooth muscle cell growth. *Chemical Communications* **49**:88, 10421. [[CrossRef](#)]
6. Ursula Schlötzer-Schrehardt, Naresh Polisetti, Johannes Menzel-Severing, Friedrich E. Kruse Tissue Engineering for Reconstruction of the Corneal Epithelium 347-360. [[CrossRef](#)]
7. Elissa K. Leonard, Vincent H. Pai, Philip Amberg, Jens Gardner, Elizabeth J. Orwin. 2012. Design and validation of a corneal bioreactor. *Biotechnology and Bioengineering* **109**:12, 3189-3198. [[CrossRef](#)]
8. Liya Shi, Rachida Aid, Catherine Le Visage, Sing Yian Chew. 2011. Biomimicking Polysaccharide Nanofibers Promote Vascular Phenotypes: A Potential Application for Vascular Tissue Engineering. *Macromolecular Bioscience* n/a-n/a. [[CrossRef](#)]
9. Lalitha Muthusubramaniam, Lily Peng, Tatiana Zaitseva, Michael Paukshto, George R. Martin, Tejal A. Desai. 2011. Collagen fibril diameter and alignment promote the quiescent keratocyte phenotype. *Journal of Biomedical Materials Research Part A* n/a-n/a. [[CrossRef](#)]